TU Delft

Delft University of Technology

Document Version
Final published version

Citation (APA)
Goetz, R. P. P. F., Van De Wouw, N., Oomen, T., Van De Wal, M. M. J., Sharif, B., & Zwart, H. J. (2025). Optimal Co-Design of Sensor Placement and State Observer for Lithography Applications. In *Proceedings of the IEEE Conference on Control Technology and Applications, CCTA 2025* (pp. 321-326). IEEE. https://doi.org/10.1109/CCTA53793.2025.11151477

Important note
To cite this publication, please use the final published version (if applicable).
Please check the document version above.

Copyright
In case the licence states "Dutch Copyright Act (Article 25fa)", this publication was made available Green Open Access via the TU Delft Institutional Repository pursuant to Dutch Copyright Act (Article 25fa, the Taverne amendment). This provision does not affect copyright ownership.
Unless copyright is transferred by contract or statute, it remains with the copyright holder.

Sharing and reuse
Other than for strictly personal use, it is not permitted to download, forward or distribute the text or part of it, without the consent of the author(s) and/or copyright holder(s), unless the work is under an open content license such as Creative Commons.

Takedown policy
Please contact us and provide details if you believe this document breaches copyrights.
We will remove access to the work immediately and investigate your claim.

This work is downloaded from Delft University of Technology.

Green Open Access added to TU Delft Institutional Repository
as part of the Taverne amendment.

More information about this copyright law amendment
can be found at https://www.openaccess.nl.

Otherwise as indicated in the copyright section:
the publisher is the copyright holder of this work and the
author uses the Dutch legislation to make this work public.

2025 IEEE Conference on Control Technology and Applications (CCTA)
August 25 - 27, 2025. San Diego, CA, USA

Optimal Co-design of Sensor Placement and State Observer for Lithography Applications

R.P.P.F. Goetz[1], N. van de Wouw[1], T. Oomen[1,3], M.M.J. van de Wal[4], B. Sharif[4], H.J. Zwart[1,2]

Abstract— **The state and output estimation accuracy depends on both the observer and the sensor locations. This paper focuses on this co-design problem in lithography applications. A theoretical formulation of this co-design problem is presented and solved for discrete-time linear stochastic models. We compare the optimal solution of two variants of the estimation problem. The first variant minimizes the transient estimation error whereas the second one minimizes the steady-state estimation error. In both cases, the Kalman filter is optimal. While solving these problems for a lithography application formulated as a 3D thermoelastic model, we observe a significant difference between the optimal sensor placements. Our results highlight the importance of designing a sensor layout in line with the desired transient or steady-state estimation performance.**

I. INTRODUCTION

Estimation and sensor placement problems arise in many control applications, an important example is in the semiconductor industry. The growing demand for performant electronic devices urges the semiconductor industry to include more and more transistors on microchips. Today, a microchip the size of a fingernail can contain tens of billions of transistors, with some features measuring only a few nanometers. The most significant limitation to further decrease the feature size occurs in lithography machines. These machines use ultraviolet (UV) light to print electronic patterns onto a silicon wafer. A chip is typically composed of many of those layers and proper alignment in between layers requires a (sub)nanometer-level positioning accuracy as explained in [1] and [2]. This accuracy is, among other, hindered by the thermal deformation of the wafer stage that holds the wafer. If known, this deformation could be compensated for in the motion loop. However, this information cannot be measured directly and thus needs to be estimated. This is achieved by placing temperature sensors on the wafer stage. Naturally, the following question arises: where to place sensors to best estimate unmeasurable variables in the system, such as these thermal-induced displacements? This is known as the sensor placement problem.

[1]R.P.P.F. Goetz, H.J. Zwart, N. van de Wouw and T. Oomen are with the Department of Mechanical Engineering, Eindhoven University of Technology, 5600 MB Eindhoven, The Netherlands (r.p.p.f.goetz@tue.nl, h.j.zwart@tue.nl, n.v.d.wouw@tue.nl, t.a.e.oomen@tue.nl)

[2]H.J. Zwart is also with the Department of Applied Mathematics, University of Twente, 7500 AE Enschede, The Netherlands

[3]T. Oomen is also with the Faculty of Mechanical Engineering, Delft University of Technology, 2600 AA Delft, The Netherlands

[4]M.M.J. van de Wal and B. Sharif are with ASML, 5504 DR Veldhoven, The Netherlands, (marc.van.de.wal@asml.com, bardia.sharif@asml.com)

Many sensor placement methods have been proposed in the literature to address a wide range of goals (see [3] or [4] for an overview). Specifically for thermal and thermoelastic processes, the authors in [5] solve an $\mathscr{H}_2$- and $\mathscr{H}_\infty$ optimization problem to position sensors and actuators for advection-diffusion equations. In [6], sensors are positioned to maximize a distinguishability measure of the error-compensation model based on modal reduction. A comparison of different model-order-reduction technics for sensor placement is presented in [7]. Other researchers considered observability-based metrics for positioning sensors [8].

In our work, we use sensor placement approaches that maximize the estimation, typically using the estimation error covariance matrix as an optimization metric. An early study was realized by Bensoussan [9] where the optimal sensor location is found by minimizing the trace of the state estimation error covariance matrix at a specific time. The more recent article [10] discusses the existence and convergence of the optimal locations for time-varying systems minimizing a similar cost. Other works such as [11] or [12] formulate the criterion on an infinite-time horizon and show that the problem is well-posed and possesses an optimal solution. Whereas the co-design in [9] – [12] fall within the Kalman filter framework (as in our paper), other researchers focused on sensor placement design with alternative observers such as functional observers [13] or reduced-order observers [14].

The specificities of our application require to answer the following question: how does the optimal sensor placement differ when optimizing the transient (finite-horizon) versus steady-state (infinite-horizon) estimation performance? This question is particularly relevant for the wafer stage system in lithography technologies because of two key features: 1) as a thermoelastic model, its thermal dynamics is slow compared to its deformation dynamics and 2) after each exposure of a wafer, which occurs every tens of seconds, the system is recalibrated, resetting the position of the wafer stage. These two elements indicate that the system never attains its steady state and that a sensor layout based on transient estimation accuracy might be more relevant than a steady-state one.

The main contribution of this paper is to clarify how the optimal sensor placement differs when based on either a transient or a steady-state estimation performance metric. To do so, we maximize the estimation accuracy of (unmeasurable) outputs through the co-design of 1) the sensor layout and 2) the observer for linear time invariant (LTI) stochastic discrete-time models. The transient estimation performance is quantified by the average variance of the error between the output and its estimate over a given time-horizon. The

2025 IEEE Conference on Control Technology and Applications (CCTA) | 979-8-3315-3908-5/25/$31.00 ©2025 IEEE | DOI: 10.1109/CCTA53793.2025.11151477

Authorized licensed use limited to: TU Delft Library. Downloaded on October 14,2025 at 09:59:48 UTC from IEEE Xplore. Restrictions apply.

steady-state estimation performance is given by the infinite-time output estimation variance.

The outline is as follows. In Section II, we formulate the general co-design problem which is later adapted for discrete-time LTI stochastic models with a linear state observer in Section III. To compare the transient and steady-state estimation performance, two approaches are defined. In both cases, the Kalman filter is used to simplify the co-design problems. Finally, the two variants of sensor placement problems are solved for a 3D thermoelastic model representing a wafer stage in lithography machines in Section IV.

Notations: A symmetric matrix $A = A^\top \in \mathbb{R}^{n\times n}$ is called positive definite if $x^\top Ax > 0$ for all $x \in \mathbb{R}^n \setminus 0$, and is written as $A \succ 0$. Similarly, the matrix A is positive semi-definite if $x^\top Ax \geq 0$ for all $x \in \mathbb{R}^n \setminus 0$, and is written as $A \succeq 0$.

A Gaussian random variable X with mean μ and variance matrix σ is written as $X \sim \mathcal{N}(\mu,\sigma)$. The expected value of the random variable X is denoted by $\mathbb{E}[X]$. Two independent random variables X and Y is denoted as $X \perp\!\!\!\perp Y$.

The signal $\hat{X}_{s|t}$ denotes an estimate of X_s at time s using measurements until time t.

The vector (spatial) differential operator is written ∇. The Laplacian operator is denoted $\Delta = \nabla\cdot\nabla$.

II. GENERAL PROBLEM FORMULATION

To formulate the co-design problem, we consider the setup illustrated in Figure 1. In this setup, Σ represents a model of the physical dynamics under study. The signal x denotes the state, which is affected by the process noise w, whereas the measurements y are influenced by the measurement noise v. The sensor layout is characterized by C and the input u is assumed to be known. The performance output z cannot be directly measured. This unmeasurable output is to be estimated via an observer O that is defined by the function g taking as inputs the time t, the signals u and y, and the known components of the model Σ_G. The estimate $\hat{z}$ of z is represented by

$$O : \hat{z} = g(t,u,y;\Sigma_G). \tag{1}$$

The freedom in the design resides in the observer O and in the measurement block C (in light gray in Fig. 1). The goal of co-design is formulated as follows.

> For the model Σ, co-design the sensor layout C and the observer O such that the output estimation accuracy is maximal.

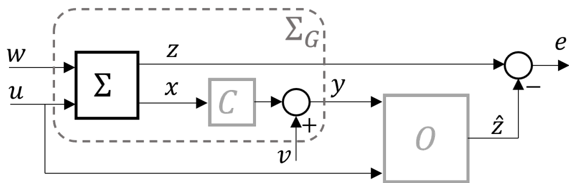

Fig. 1. Block scheme of the estimation system. The model Σ_G is the combination of Σ and C. The estimation error signal $e = z-\hat{z}$.

The estimation accuracy is quantified by the estimation error $e = z-\hat{z}$. The function $f(e)$ defines the optimality metric. Depending on the application, the sensor design C is limited by the type of sensors, the available locations, etc. This constraint is expressed as $C \in \Omega_C$. Similarly, the observer design is restricted to a specific class of observers denoted Ω_g, i.e., g in (1) is an element of Ω_g. Finally, the goal is formulated as an optimization problem:

$$\min_{C\in\Omega_C,\, g\in\Omega_g} f(e). \tag{2}$$

The formulation (2) is still very general. Three elements have still to be chosen: the cost function f, and the sensor class Ω_C and observer class Ω_g. Specific choices of the cost function and observer are typically guided by the characteristics of the system and signals, such as whether they are linear or nonlinear, stochastic or deterministic, as well as the application under study. In the next section, we choose f and Ω_g for a discrete-time LTI stochastic model.

III. PROBLEM FORMULATION FOR STOCHASTIC MODELS

In this section, the co-design problem is formulated for discrete-time LTI stochastic models by choosing the observer class Ω_g and cost functions f. Two optimization problems are defined to capture the difference between the minimization of the transient and the steady state estimation error.

A. Discrete-time LTI stochastic model

The following class of discrete-time LTI systems is considered:

$$\Sigma_G := \begin{bmatrix} x_{k+1} \\ y_k \\ z_k \end{bmatrix} = \begin{bmatrix} A & B_u & B_w & 0 \\ C & 0 & 0 & I \\ L & 0 & 0 & 0 \end{bmatrix} \begin{bmatrix} x_k \\ u_k \\ w_k \\ v_k \end{bmatrix}, \tag{3}$$

with k the discrete time index. Note that we assume that our sensor configuration can be represented by the matrix C. The disturbance w and the measurement noise v in (3) are zero-mean Gaussian white noises and the initial state x_0 is a Gaussian random variable:

$$w_k \sim \mathcal{N}(0,Q), \quad v_k \sim \mathcal{N}(0,R), \quad x_0 \sim \mathcal{N}(\hat{x}_{0|0},P_{0|0}) \tag{4}$$

with known symmetric covariance matrices $Q \succeq 0$, $R \succ 0$, $P_{0|0} \succeq 0$ and known initial estimate $\hat{x}_{0|0}$. The initial state and noises are assumed to be mutually independent

$$x_0 \perp\!\!\!\perp w_0 \perp\!\!\!\perp \ldots \perp\!\!\!\perp w_k \perp\!\!\!\perp v_1 \perp\!\!\!\perp \ldots \perp\!\!\!\perp v_k. \tag{5}$$

For simplicity, Σ_G in (3) is assumed to be asymptotically stable. The definition of the constraint $C \in \Omega_C$ relates to the sensor type used for the application, see Section IV.

B. Finite- and infinite-horizon cost functions

After defining the class of system in the previous subsection, we define the cost function f in (2) using the expected value of the squared norm of the output estimation error:

$$\mathbb{E}\left[\|e_k\|^2\right] = \mathbb{E}\left[(z_k-\hat{z}_{k|k})^\top(z_k-\hat{z}_{k|k})\right]. \tag{6}$$

Authorized licensed use limited to: TU Delft Library. Downloaded on October 14,2025 at 09:59:48 UTC from IEEE Xplore. Restrictions apply.

Two distinct minimization problems are defined to capture the difference between the transient and steady-state estimation performance:

- The finite-horizon co-design problem
$$\min_{C\in\Omega_C}\min_{g\in\Omega_g}\frac{1}{k_f}\sum_{k=1}^{k_f}\mathbb{E}\left[\|e_k\|^2\right], \tag{7}$$
where the cost function measures the average estimation error on the interval $[1,k_f]$, i.e., transient output estimation accuracy.
- The infinite-horizon co-design problem
$$\min_{C\in\Omega_C}\min_{g\in\Omega_g}\lim_{k\to\infty}\mathbb{E}\left[\|e_k\|^2\right], \tag{8}$$
where the cost function measures the infinite-time or steady-state output estimation accuracy.

Note that the global minimization in (2) has been written as a nested minimization in (7) and (8). This follows from the remark below.

Remark 3.1: Let a function $f: X\times Y\mapsto[0,\infty); (x,y)\mapsto f(x,y)$ then,
$$\inf_{x\in X}\left(\inf_{y\in Y}f(x,y)\right)=\inf_{x\in X,y\in Y}f(x,y). \tag{9}$$
Proof: Denote,
$$L:=\inf_{x\in X}\left(\inf_{y\in Y}f(x,y)\right),\quad R:=\inf_{x\in X,y\in Y}f(x,y). \tag{10}$$
By definition of the infimum, it holds that
$$g(x):=\inf_{y\in Y}f(x,y)\geq R \tag{11}$$
and $\forall\varepsilon>0,\exists(x_0,y_0)\in(X,Y)$ such that $f(x_0,y_0)\leq R+\varepsilon$. Then,
$$R\leq\inf_{x\in X}g(x)=L,\quad L\leq f(x_0,y_0)\leq R+\varepsilon. \tag{12}$$
Therefore, since ε can be chosen arbitrarily small, $L=R$. ■ Note that if the infima are attained, they can be written as minima. This is actually the case with the observer structure presented in the next subsection.

C. Observer

The estimator class Ω_g consists of all functions g of past inputs and measurements,
$$\hat{z}_{k|k}=g(k,u_0,\dots,u_k,y_1,\dots,y_k). \tag{13}$$
By Lemma 2.5 in [15] or Theorem 5.5 in [16], we have that the estimator (13) which minimizes $\mathbb{E}[\|z_k-\hat{z}_{k|k}\|^2]$ is given by $\mathbb{E}[z_k|u_0,\dots,u_k,y_1,\dots,y_k]$. From [17], it can also be concluded that it minimizes
$$\sum_{k=1}^{k_f}\mathbb{E}\left[(z_k-\hat{z}_{k|k})^\top(z_k-\hat{z}_{k|k})\right]. \tag{14}$$
Since $z_k=Lx_k$ in (3), we have that
$$\hat{z}_{k|k}=L\mathbb{E}[x_k|u_0,\dots,u_k,y_1,\dots,y_k]:=L\hat{x}_{k|k}. \tag{15}$$
It is well known that the optimal $\hat{x}_{k|k}$ is given by the Kalman filter [15]. Its dynamics is given, for $k=0,1,\dots,$ by
$$\hat{x}_{k+1|k}=A\hat{x}_{k|k}+B_uu_k,\quad \hat{y}_{k+1|k}=C\hat{x}_{k+1|k} \tag{16}$$
$$\hat{x}_{k+1|k+1}-\hat{x}_{k+1|k}=K_{k+1}(y_{k+1}-\hat{y}_{k+1|k}) \tag{17}$$
with K_{k+1} the observer gain. Equation (16) is the prediction step where the *a priori* state estimate $\hat{x}_{k+1|k}$ and measurement estimate $\hat{y}_{k+1|k}$ are computed using only measurements (and inputs) until time k. These expressions are directly based on the (known part of the) system dynamics. Equation (17) is the update step where the *a priori* estimate is corrected using the measurement y_{k+1} at time $k+1$ to find the *a posteriori* state estimate $\hat{x}_{k+1|k+1}$. The error covariance matrices of the measurement, the *a priori* and *a posteriori* state error covariance matrices are
$$\begin{aligned}S_k&=\mathbb{E}[(y_k-\hat{y}_{k|k-1})(y_k-\hat{y}_{k|k-1})^\top]\\&=CP_{k|k-1}C^\top+R, &(18)\\P_{k+1|k}&=\mathbb{E}[(x_{k+1}-\hat{x}_{k+1|k})(x_{k+1}-\hat{x}_{k+1|k})^\top]\\&=AP_{k|k}A^\top+B_wQB_w^\top, &(19)\\P_{k+1|k+1}&=\mathbb{E}[(x_{k+1}-\hat{x}_{k+1|k+1})(x_{k+1}-\hat{x}_{k+1|k+1})^\top]\\&=(K_{k+1}-P_{k+1|k}C^\top S_{k+1}^{-1})S_{k+1}(K_{k+1}-P_{k+1|k}C^\top S_{k+1}^{-1})^\top &(20)\\&\quad-P_{k+1|k}C^\top S_{k+1}^{-1}CP_{k+1|k}+P_{k+1|k},\\&=-P_{k+1|k}C^\top S_{k+1}^{-1}CP_{k+1|k}+P_{k+1|k} &(21)\end{aligned}$$
with the observer gain
$$K_{k+1}=P_{k+1|k}C^\top S_{k+1}^{-1}. \tag{22}$$
From (15) and (20), the error covariance matrix of the output z is
$$P_{z_{k|k}}=\mathbb{E}[(z_k-\hat{z}_{k|k})(z_k-\hat{z}_{k|k})^\top]=LP_{k|k}L^\top. \tag{23}$$
From (6), (23) and the cyclic permutation property of the trace, we observe that
$$\begin{aligned}\mathbb{E}\left[\|e_k\|^2\right]&=\mathbb{E}\left[(z_k-\hat{z}_{k|k})^\top(z_k-\hat{z}_{k|k})\right]\\&=\mathrm{tr}\left[\mathbb{E}\left[(z_k-\hat{z}_{k|k})(z_k-\hat{z}_{k|k})^\top\right]\right]\\&=\mathrm{tr}\left[P_{z_{k|k}}\right]\\&=\mathrm{tr}\left[LP_{k|k}L^\top\right]. &(24)\end{aligned}$$
Since the Kalman filter (16) – (22) is the best observer for the first minimization in (7) and (8), the problems are rewritten using (24) and the Kalman filter design:

- The finite-horizon problem (7) becomes
$$\begin{aligned}&\min_{C\in\Omega_C}\frac{1}{k_f}\sum_{k=1}^{k_f}\mathrm{tr}[LP_{k|k}L^\top],\\&\quad P_{k|k}=-P_{k|k-1}C^\top S_k^{-1}CP_{k|k-1}+P_{k|k-1},\\&\quad K_k=P_{k|k-1}C^\top S_k^{-1}.\end{aligned}\tag{25}$$

Authorized licensed use limited to: TU Delft Library. Downloaded on October 14,2025 at 09:59:48 UTC from IEEE Xplore. Restrictions apply.

- The infinite-horizon problem (8) becomes

$$\begin{aligned}&\min_{C\in\Omega_C}\lim_{k\to\infty}\mathrm{tr}[LP_{k|k}L^\top]=\min_{C\in\Omega_C}\mathrm{tr}[L\tilde{P}L^\top],\\&\quad\tilde{P}=P-KCP,\\&\quad P=APA^\top-APC^\top(CPC^\top+R)^{-1}CPA^\top\\&\qquad+B_wQB_w^\top,\\&\quad K=PC^\top(CPC^\top+R)^{-1},\end{aligned}\tag{26}$$

  with P the *a priori* steady-state error covariance matrix. We observe that P is the solution of a discrete-time algebraic Riccati equation. The *a posteriori* steady-state error covariance matrix $\tilde{P}$ is simply the update of P and K is the steady-state gain.

Note that estimating the output via the state is a choice. Another way to estimate directly the output could have been chosen. In (25) and (26), only the sensor layout optimization remains. In the following, we solve the two problems for the lithography application and compare the results.

IV. SENSOR LAYOUT OPTIMIZATION FOR A LITHOGRAPHY APPLICATION

In this section, the problem of placing optimally a unique sensor for a 3D thermoelastic system is addressed.

A. Thermoelastic model of a wafer stage

The wafer stage is modeled as a rectangular block of stainless steel of dimension $0.3\times0.3\times0.05$ in meters. The corresponding spatial domain is denoted as Ξ. The material is isotropic with the following parameters: density $\rho=7850\ \mathrm{kg/m^3}$, heat capacity $c_p=420\ \mathrm{J/kg\,K}$, thermal conductivity $\kappa=45\ \mathrm{W/K\,m}$ and coefficient of thermal expansion $\alpha=11\cdot10^{-6}\ \mathrm{m/K}$. The basic heat conservation law is

$$-\nabla\cdot q=c_p\rho\frac{\partial\theta}{\partial t},\qquad t\geq0,\xi\in\Xi\tag{27}$$

with $\theta(t,\xi)$ the temperature variation of the object from the environment temperature $T_\infty=295.15$ K, $\theta=T-T_\infty$, $q(t,\xi)$ the heat flux and $\xi\in\Xi$ the spatial coordinate. Fourier's law of thermal conduction states that $q=-\kappa\nabla\theta$. Therefore, the heat conduction equation is given by

$$\kappa\Delta\theta=c_p\rho\frac{\partial\theta}{\partial t},\qquad t\geq0,\xi\in\Xi.\tag{28}$$

The partial differential equation (28) is complete when boundary conditions and initial conditions are given. The boundary of Ξ is split into two non-overlapping parts, i.e. $\partial\Xi=\partial\Xi_u\cap\partial\Xi_h$. On $\partial\Xi_u$, boundary surface heat supply conditions are taken:

$$n^\top q=-q_u,\qquad t\geq0,\xi\in\partial\Xi_u\tag{29}$$

with n the normal to the surface(s) and q_u the heat load in $\mathrm{W/m^2}$ applied on $\partial\Xi_u$. The boundary $\partial\Xi_u$ contains areas where heat is induced by the UV exposure, by the actuators used for positioning the stage and by the motion table below the wafer stage, as illustrated in Figure 2. On $\partial\Xi_h$, convective heat transfer boundary conditions are assumed:

$$n^\top q=h(T-T_\infty)=h\theta,\qquad t\geq0,\xi\in\partial\Xi_h\tag{30}$$

with the heat transfer coefficient between steel and air $h=7.9\ \mathrm{W/K\,m^2}$. A zero initial condition is taken. In this study, the displacement is only caused by temperature variations. Hence, the thermal strain is defined as

$$\varepsilon=\alpha(T-T_\infty)=\alpha\theta.\tag{31}$$

We consider to have a zero strain and displacement at temperature $T=T_\infty$. The strain-displacement relation gives

$$\varepsilon=\nabla\gamma,\qquad t\geq0,\xi\in\Xi\tag{32}$$

with $\gamma(t,\xi)$ the thermal-induced displacement field.

The continuous-time model composed by Equations (27) – (32) is discretized in space using the finite element method (Chapter 3 in [18], [19]) and in time via the zero-order-hold method with time step $\Delta t=0.1$ s in such a way that the system remains stable with a well-chosen time step regarding the time constant of the system. The spatial domain is divided into 6 linear hexahedron elements for the x and y axis and into 4 elements along the z axis resulting in 144 hexahedrons and $N=245$ nodes (see Figure 2). Adding the two stochastic perturbations v and w, the resulting discrete-time state-space representation is as in (3)

$$\begin{aligned}x_{k+1}&=Ax_k+Bu_k+Bw_k\\y_k&=Cx_k+v_k\\z_k&=Lx_k\end{aligned}\tag{33}$$

with $x_k\in\mathbb{R}^N$ the temperature variation field containing all the nodal temperature variation $\theta(t_k,\xi_i)$ at time t_k and at all discretized positions $\xi_i\in\Xi$, $i\in\{1,\ldots,N\}$, u_k the known heat loads, w_k the heat disturbances, v_k the measurement noise, z_k the thermal-induced displacement at specific locations, typically at the position sensors (encoders). Note that we consider each heat load of $\partial\Xi_u$ to be composed of two parts: a nominal known heat load u and an unknown heat disturbance w. Thus, they are on top of one another, i.e., comparing to (3) we have $B_w=B_u=B$. The signals w_k, v_k, x_0 are defined as in (4) with $\hat{x}_{0|0}=0$. The heat load u_k (as well as the disturbance w_k) has 6 components, one heat load coming from the UV exposure, one from the motion table below the wafer stage and four from actuators (Figure 2).

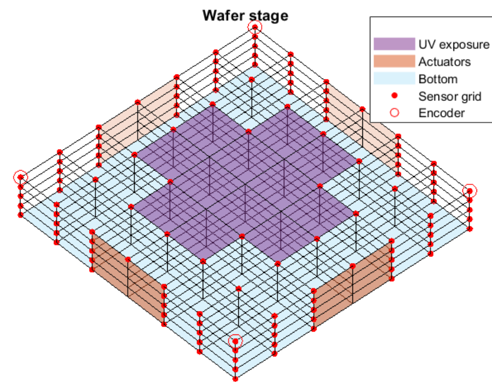

Fig. 2. Setup of the discretized wafer stage model. The boundary $\partial\Xi_u$ contains the area of the UV exposure (purple), the actuators (orange) and the bottom of the wafer stage (light blue).

Authorized licensed use limited to: TU Delft Library. Downloaded on October 14,2025 at 09:59:48 UTC from IEEE Xplore. Restrictions apply.

The C matrix represents a point sensor at one of the 124 available discretized positions (red dots in Figure 2 that form the set Ω_C). Those candidate locations are defined on the surface of the wafer stage because placing sensors inside the wafer stage or between components (actuators, wafer, ...) is unfeasible. The sensor has an accuracy range of $\pm 0.001\,\text{K}$, which corresponds to a noise variance $R = 10^{-6}\,\text{K}^2$.

The heat power of the disturbances associated with the exposure load, the bottom load and the four actuators (left, front, right, back) are assumed with 68% confidence to lie between $\pm 7W, \pm 1W, \pm 5\,\text{W}$, respectively. Using the empirical rule of normal distributions and the disturbance areas, we find the covariance matrix, $Q = \text{diag}([0.054\ 0.0001\ 1\ 1\ 1\ 1] \cdot 10^6)\,(\text{W}/\text{m}^2)^2$. The covariance matrix of the initial state $P_{0|0}$ is assumed to be diagonal with zero entries at nodes part of the actuator surfaces and $0.05\,\text{K}^2$ elsewhere. This is because the actuators are cooled down and, therefore, the temperature at the actuators can initially be estimated accurately.

B. Results

The finite- (25) and infinite-horizon problems (26) are solved using a brute force algorithm, i.e., the cost functions are evaluated for all sensor configurations. Several horizon lengths, $k_f \in \{2, 20, 100, 500, 10000\}$, are used for the finite-horizon problem. The Table I presents the evolution of the optimal sensor location (column 2) with the horizon (column 1). The optimal cost is given in column 3 and is compared to the one at $\circ$ (column 4), which is the infinite-horizon optimal location. Figure 3 shows the locations on the wafer stage.

The table and figure show that the optimal sensor location changes with the considered horizon. Initially, the optimal sensor is placed between the UV exposure and the actuator at $+$, $\times$ or $\square$. For longer horizons, the optimal location tends toward the one of the infinite-horizon, positioned near the UV exposure load/disturbance at $\circ$. The two last columns show the cost difference of the k_f-horizon problems for the optimal sensor and for the infinite-horizon optimal sensor $\circ$.

C. Discussion

The results presented in section IV-B show a clear change in optimal sensor location with the horizon of the optimization problem. In other words, depending on whether the transient estimation performance or the steady-state estimation performance is optimized, the optimal sensor location shifts. For instance, if the best estimation performance is desired during the ten first seconds ($k_f = 100$), the sensor should be positioned at $\times$ and not at the infinite-horizon optimal location $\circ$ (line $k_f = 100$ in Table I). By definition, the cost is the sum of variances of the displacement estimation error. In total there are 12 variances because of 3 displacement directions for 4 encoders. Using the empirical rule of normal distributions, the average estimation error per encoder is of $\pm 185\,\text{nm}$ for $\times$ and $\pm 186.6\,\text{nm}$ for $\circ$. Thus, there is an estimation gain of $1.6\,\text{nm}$ by positioning the sensor at $\times$ instead of $\circ$ for a ten-seconds horizon. At first sight, this difference may seem small. However, in chip manufacturing, the exposure needs to be accurate within sub-nanometer levels. A large estimation error of the displacement at each encoder causes inaccurate positioning of the wafer stage resulting in a lower exposure precision. Hence, this estimation difference of $1.6\,\text{nm}$ is in that case significant.

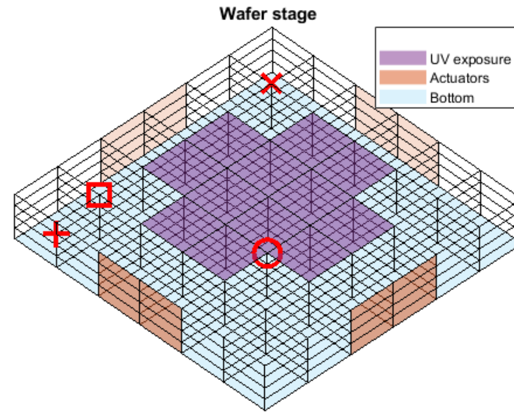

Fig. 3. Optimal sensor locations at $\{+, \square, \times, \times, \circ\}$ for horizons $k_f \in \{2, 20, 100, 500, 10000\}$, respectively (See Table I).

Besides the time horizon k_f, the optimal sensor layout depends on all the parameters of the system dynamics. We discuss a few of them and their expected effect on the optimal sensor layout. If the initial state uncertainty $P_{0|0}$ is high, we expect the optimal sensor, for short-time performance, to be located where the initial uncertainty is maximal. For long and infinite horizon, this optimal location will not depend on $P_{0|0}$. Therefore, determining the initial uncertainty is essential for slow systems active on a short horizon. In industry, defining this initial covariance is usually challenging and sometimes impossible. This is one of the reasons why engineers mainly use infinite-horizon techniques to place sensors.

Another parameter that will impact the optimal sensor placement is the disturbance noise, characterized by Q. For short-time estimation performance, it might be better to position the sensor at a location that is affected by a dominant disturbance. For long-time horizon, it can be that the optimal location is a trade-off between all the disturbances to obtain as much information on the uncertainties as possible. However, this is not always the case. Similarly as for $P_{0|0}$, determining the matrix Q can be challenging. Moreover, we considered white noise disturbances whereas in the industry, noise might not always be of this nature.

Other system characteristics can impact the optimal sensor

TABLE I
SOLUTIONS OF THE FINITE- AND INFINITE-HORIZON PROBLEMS WITH THE SYMBOLS CORRESPONDING TO THOSE IN FIGURE 3

Horizon k_f	Optimal sensor location	Optimal cost	Cost of $\circ$
2	$+$	$1.54 \cdot 10^{-13}$	$1.55 \cdot 10^{-13}$
20	$\times$	$1.42 \cdot 10^{-13}$	$1.43 \cdot 10^{-13}$
100	$\times$	$1.02 \cdot 10^{-13}$	$1.04 \cdot 10^{-13}$
500	$\square$	$4.44 \cdot 10^{-14}$	$4.60 \cdot 10^{-14}$
10000	$\circ$	$8.04 \cdot 10^{-15}$	
∞	$\circ$	$2.19 \cdot 10^{-15}$	

Authorized licensed use limited to: TU Delft Library. Downloaded on October 14,2025 at 09:59:48 UTC from IEEE Xplore. Restrictions apply.

layout such as the location of the disturbances B_w, the output parametrized by L, the sensor noise characterized by R, and the number of sensors. In this work, the disturbance areas were fixed to the ones of the inputs. It seems logical to do so, because there is still uncertainty regarding the input that can be modeled as disturbances. However, those disturbance areas could be slightly different. For instance, the disturbance area of the exposure could be slightly more than the exposure area itself because some fraction of light could still strike just outside this area. Regarding the sensor, the noise covariance is directly defined by the type of sensor used. A trade-off between the precision and the number of the sensors used is possible as shown in [11].

V. CONCLUSIONS AND FUTURE WORK

A. Conclusions

In this paper, the co-design problem of sensor placement and observer for maximizing the output estimation performance is studied for stable LTI stochastic discrete-time models. Two optimization problems were formulated: a finite-horizon and an infinite-horizon one (Section III-B). By means of a 3D thermoelastic model for a lithography application, we show that the optimal sensor location depends on the time horizon on which we want to maximize the estimation performance (Section IV). Our results highlight the importance of designing a sensor layout in line with the terminal time by which maximum estimation performance is desired. For achieving the best transient estimation performance, engineers should apply finite-horizon techniques for sensor placement, as this can significantly improve the performance of various technologies as illustrated here for lithography in chip manufacturing.

B. Future Work

As discussed in Section IV-C, the optimal sensor placement depends on many elements. A deeper study on their impact on the sensor placement for lithography applications should be done, especially regarding the number of sensors: what is the estimation gain by adding one or more sensors?

On the algorithmic side, the sensor placement problem is here solved by a brute force algorithm. The considered cost functions have been shown to not have modularity properties [20]. In other words, the contribution to the cost for adding one sensor to the configuration is independent to the cost of the current configuration. Therefore, optimization approaches based on modularity properties are excluded whereas they can be used for observability-based cost functions having this property (see Chapter 3 in [21]). In addition, placing the sensor by minimizing error covariance matrix is an NP-hard problem [20]. For all these reasons, a study should focus on improving the algorithm/approach for solving the multiple sensor placement problem.

ACKNOWLEDGMENT

This research is part of the project ThermOpt D&C that is co-financed by Holland High Tech, top sector High-Tech Systems and Materials, with a PPP innovation subsidy for public-private partnerships for research and development.

REFERENCES

[1] H. Butler, "Position Control in Lithographic Equipment [Applications of Control]," *IEEE Control Systems Magazine*, vol. 31, pp. 28–47, Oct. 2011. Conference Name: IEEE Control Systems Magazine.

[2] M. Heertjes, H. Butler, N. Dirkx, S. van der Meulen, R. Ahlawat, K. O'Brien, J. Simonelli, K.-T. Teng, and Y. Zhao, "Control of Wafer Scanners: Methods and Developments," in *2020 American Control Conference (ACC)*, pp. 3686–3703, July 2020. ISSN: 2378-5861.

[3] V. Gupta, M. Sharma, and N. Thakur, "Optimization Criteria for Optimal Placement of Piezoelectric Sensors and Actuators on a Smart Structure: A Technical Review," *Journal of Intelligent Material Systems and Structures*, vol. 21, pp. 1227–1243, Aug. 2010. Publisher: SAGE Publications Ltd STM.

[4] M. van de Wal and B. de Jager, "A review of methods for input/output selection," *Automatica*, vol. 37, pp. 487–510, Apr. 2001.

[5] D. Veldman, R. Fey, H. Zwart, M. van de Wal, J. van den Boom, and H. Nijmeijer, "Sensor and actuator placement for proportional feedback control in advection-diffusion equations," *IEEE Control Systems Letters*, vol. 4, pp. 193–198, Jan. 2020.

[6] A. H. Koevoets, H. J. Eggink, J. van der Sanden, J. Dekkers, and T. A. M. Ruijl, "Optimal sensor configuring techniques for the compensation of thermo-elastic deformations in high-precision systems," in *2007 13th International Workshop on Thermal Investigation of ICs and Systems (THERMINIC)*, pp. 208–213, Sept. 2007.

[7] P. Benner, R. Herzog, N. Lang, I. Riedel, and J. Saak, "Comparison of model order reduction methods for optimal sensor placement for thermo-elastic models*," *Engineering Optimization*, vol. 51, pp. 465–483, Mar. 2019.

[8] M. Wrobel and T. Meurer, "Optimal sensor placement and estimator-based temperature control for a deep drawing process," *Journal of Process Control*, vol. 124, pp. 92–104, Apr. 2023.

[9] A. Bensoussan, "Optimization of sensors' location in a distributed filtering problem," in *Stability of Stochastic Dynamical Systems* (R. F. Curtain, ed.), Lecture Notes in Mathematics, (Berlin, Heidelberg), pp. 62–84, Springer, 1972.

[10] X. Wu, B. Jacob, and H. Elbern, "Optimal Control and Observation Locations for Time-Varying Systems on a Finite-Time Horizon," *SIAM Journal on Control and Optimization*, vol. 54, pp. 291–316, Jan. 2016. Publisher: Society for Industrial and Applied Mathematics.

[11] M. Zhang and K. Morris, "Sensor Choice for Minimum Error Variance Estimation," *IEEE Transactions on Automatic Control*, vol. 63, pp. 315–330, Feb. 2018.

[12] S.-X. Tang and K. A. Morris, "Optimal sensor design for infinite-time Kalman filters," in *2017 IEEE 56th Annual Conference on Decision and Control (CDC)*, pp. 64–69, Dec. 2017.

[13] M. Demetriou, "Robust sensor location optimization in distributed parameter systems using functional observers," in *Proceedings of the 44th IEEE Conference on Decision and Control*, pp. 7187–7192, Dec. 2005. ISSN: 0191-2216.

[14] A. A. Alonso, I. G. Kevrekidis, J. R. Banga, and C. E. Frouzakis, "Optimal sensor location and reduced order observer design for distributed process systems," *Computers & Chemical Engineering*, vol. 28, pp. 27–35, Jan. 2004.

[15] P. R. Kumar and P. P. Varaiya, *Stochastic Systems: Estimation, Identification, and Adaptive Control*. Prentice Hall, 1986.

[16] G. Gu, *Discrete-Time Linear Systems: Theory and Design with Applications*. Springer Science & Business Media, Feb. 2012.

[17] J. L. Speyer and W. H. Chung, *Stochastic Processes, Estimation, and Control*. Advances in Design and Control, Society for Industrial and Applied Mathematics, Jan. 2008.

[18] R. W. Lewis, P. Nithiarasu, and K. N. Seetharamu, *Fundamentals of the Finite Element Method for Heat and Fluid Flow*. Wiley, 1 ed., Apr. 2004.

[19] G. Dhondt, *The Finite Element Method for Three-Dimensional Thermomechanical Applications*. Chichester: Wiley, 1st edition ed., June 2004.

[20] H. Zhang, R. Ayoub, and S. Sundaram, "Sensor selection for Kalman filtering of linear dynamical systems: Complexity, limitations and greedy algorithms," *Automatica*, vol. 78, pp. 202–210, Apr. 2017.

[21] R. W. H. Merks, *Towards control relevant system design and constrained order controller synthesis: with a thermal control application in immersion lithography*. Phd Thesis, Technische Universiteit Eindhoven, Eindhoven, Sept. 2019. ISBN: 9789038648361.

Authorized licensed use limited to: TU Delft Library. Downloaded on October 14,2025 at 09:59:48 UTC from IEEE Xplore. Restrictions apply.